

Lattice distortions, incommensurability, and stripes in the electronic model for high- T_c cuprates

Takashi Yanagisawa, Mitake Miyazaki, Shigeru Koikegami, Soh Koike and Kunihiro Yamaji
 Nanoelectronics Research Institute, National Institute of Advanced Industrial Science and Technology (AIST),
 Central 2, 1-1-1 Umezono, Tsukuba, Ibaraki 305-8568, Japan

(Dated: May 6, 2018)

Striped superconductivity (SC) with lattice distortions is investigated based on the three-band Hubbard model for high- T_c cuprates. A stable inhomogeneous striped state is determined in the low-temperature tetragonal (LTT) phase with lattice distortions using a quantum variational Monte Carlo method. The ground state has vertical or horizontal hole-rich arrays coexisting with incommensurate magnetism and SC induced by several percents of lattice deformations. The SC order parameter oscillates according to the inhomogeneity in the antiferromagnetic background with its maximums in the hole-rich regions, and the SC condensation energy is reduced as the doping rate decreases.

PACS numbers: 78.20.-e, 78.30.-j, 74.76.Bz

Over the last decade the oxide high- T_c superconductors have been investigated intensively.[1] The mechanism of superconductivity (SC) has been extensively studied using various two-dimensional (2D) models of electronic interactions. The 2D three-band Hubbard model is the simple and most fundamental model among such models. The 2D one-band Hubbard model is regarded as the simplified model of the three-band model. Studies of these models over the last decade indicated that the d -wave SC is induced from the electronic repulsive interaction[2, 3, 4, 5, 6, 7, 8]; significantly it has been

shown that the SC condensation energy and the magnitude of order parameter are in reasonable agreement with the experimental results in the optimally doped case.[9, 10, 11]

The SC condensation energy obtained by the variational Monte Carlo method (VMC) is estimated as $E_{cond} \simeq 0.00117t = 0.59\text{meV}$ per site in the optimally doped case for the single-band Hubbard model in the bulk limit.[6, 9] We must note that E_{cond} is given as $0.17 \sim 0.26\text{meV}$ by specific heat data[12, 13] and 0.26meV by the critical magnetic field value $H_c^2/8\pi$ [14]. The agreement of the VMC value with the experimental estimation is quite significant and supports the calculations. The VMC method can be regarded as an approximation to Quantum Monte Carlo calculations.[15, 16] The SC order parameter Δ_s determined from a minimum of the energy is of the order of $0.01 \sim 0.015 = 15\text{meV} \sim 20\text{meV}$ at hole density $\delta \sim 0.2$. [11]

The interplay between magnetism and superconductivity is suggested in the underdoped region. The reduction of T_c in this region remains unresolved and may be related to magnetism. An existence of incommensurate correlations with modulation vectors given by $Q_s = (\pi \pm 2\pi\delta, \pi)$ and $Q_c = (\pm 4\pi\delta, 0)$ (or $Q_s = (\pi, \pi \pm 2\pi\delta)$ and $Q_c = (0, \pm 4\pi\delta)$) has been suggested for the hole-doping rate δ . [17, 18, 19, 20, 21, 22, 23] The linear doping dependence of incommensurability in the underdoped region supports a striped structure and suggests a relationship between magnetism and SC.[19] A relationship between the SDW, CDW orders and a crystal structure is also suggested in intensive studies by the neutron-scattering measurements:[17, 24, 25, 26] in particular in the low-temperature tetragonal (LTT) and low-temperature less-orthorhombic (LTLO) phases, the CDW order is stabilized,[27] while no well defined incommensurate CDW peaks were observed for the orthorhombic systems.[25, 26] In the elastic and inelastic neutron scattering experiments with $\text{La}_{2-x}\text{Sr}_x\text{CuO}_4$, the incommensurate magnetic scattering spots around (π, π) have been observed in the SC phase in the range of

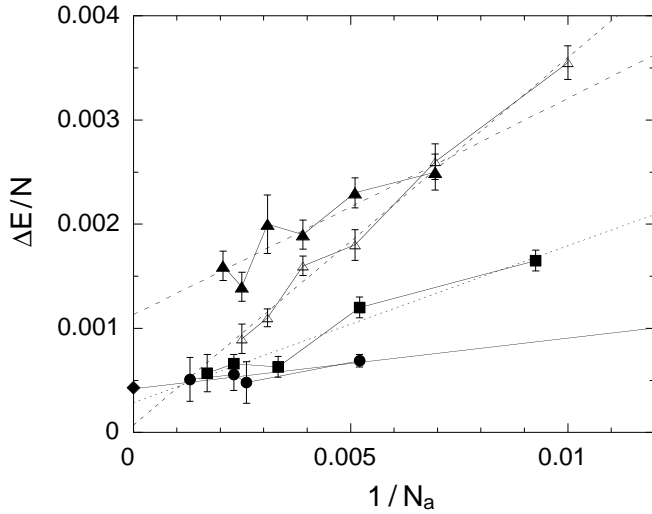


FIG. 1: SC condensation energy per site as a function of $1/N_a$ in t units where $t \approx t_{pd}/3$ and N_a is the number of atoms. Squares are for $\delta \approx 0.2$, $t_{pp}/t_{pd} = 0.4$ and $U_d/t_{pd} = 8$ for the three-band model on square lattices. Circles are at $\delta = 1/8$ coexisting with stripes for $t_{pp}/t_{pd} = 0.4$ and $U_d/t_{pd} = 8$ on rectangular lattices 32×8 , 24×6 , 16×8 and 16×4 . Triangles are for the single-band Hubbard model; $\delta = 0.86$ and $t' = -0.2$ and $U = 8$ for solid symbols and $\delta = 0.84$ and $t' = -0.15$ for open symbols (energy unit is t). [9] The diamond shows the value indicated from experiments.

$0.05 < x < 0.13$. [19, 26, 28]

In this paper an incommensurate striped SC under lattice distortions is investigated based on the three-band model. In the description of SC in the underdoped region it is of prime importance to investigate the effect of inhomogeneity. In this paper we take into account all of the inhomogeneity, lattice instability and anisotropic pairing to clarify the ground state in the underdoped region of high- T_c cuprates. The Hamiltonian is given by $H = H_{pd}^0 + V + H_{el}$ where

$$\begin{aligned}
H_{pd}^0 = & \epsilon_d \sum_{i\sigma} d_{i\sigma}^\dagger d_{i\sigma} + \epsilon_p \sum_{i\sigma} (p_{i+\hat{x}/2,\sigma}^\dagger p_{i+\hat{x}/2,\sigma} \\
& + p_{i+\hat{y}/2,\sigma}^\dagger p_{i+\hat{y}/2,\sigma}) + t_{pd} \sum_{i\sigma} [d_{i\sigma}^\dagger (p_{i+\hat{x}/2,\sigma} + p_{i+\hat{y}/2,\sigma} \\
& - p_{i-\hat{x}/2,\sigma} - p_{i-\hat{y}/2,\sigma}) + h.c.] \\
& + t_{pp} \sum_{i\sigma} (1 + v_i) [p_{i+\hat{y}/2,\sigma}^\dagger p_{i+\hat{x}/2,\sigma} - p_{i+\hat{y}/2,\sigma}^\dagger p_{i-\hat{x}/2,\sigma} \\
& - p_{i-\hat{y}/2,\sigma}^\dagger p_{i+\hat{x}/2,\sigma} + p_{i-\hat{y}/2,\sigma}^\dagger p_{i-\hat{x}/2,\sigma} + h.c.] \\
& + t_{pd} \sum_{i\sigma} [u_{i\hat{x}} d_{i\sigma}^\dagger p_{i+\hat{x}/2,\sigma} - u_{i,-\hat{x}} d_{i\sigma}^\dagger p_{i-\hat{x}/2,\sigma} \\
& + u_{i\hat{y}} d_{i\sigma}^\dagger p_{i+\hat{y}/2,\sigma} - u_{i,-\hat{y}} d_{i\sigma}^\dagger p_{i-\hat{y}/2,\sigma} + h.c.], \quad (1)
\end{aligned}$$

$$V = U_d \sum_i d_{i\uparrow}^\dagger d_{i\uparrow} d_{i\downarrow}^\dagger d_{i\downarrow}, \quad (2)$$

where H_{el} denotes the lattice elastic energy given by $H_{el} = (K_{pd}/2) \sum_i (u_{i\hat{x}}^2 + u_{i,-\hat{x}}^2 + u_{i\hat{y}}^2 + u_{i,-\hat{y}}^2) + (K_{pp}/2) \sum_i 4v_i^2$ where K_{pd} and K_{pp} denote the elastic constants. \hat{x} and \hat{y} represent unit vectors in the x - and

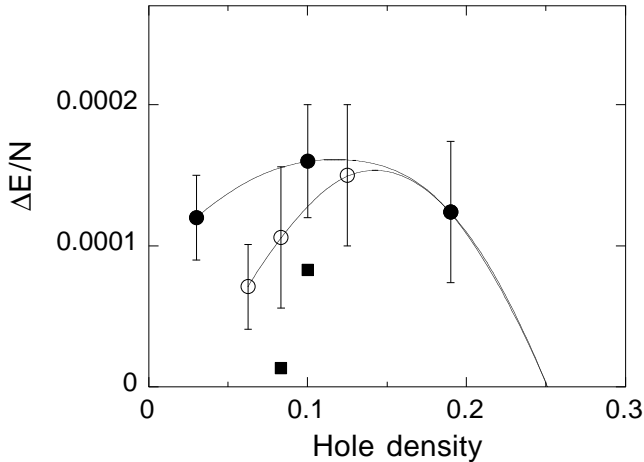


FIG. 2: SC condensation energy per site vs the hole density in t_{pd} units, where the parameters are $t_{pp} = 0.4$ and $U_d = 8$. Solid circles and open circles indicate the SC condensation energy for the uniform SC and striped SC, respectively. The lines are fitted by parabola. Squares are obtained for the single-band Hubbard model with the next-nearest transfer $t' = -0.2$ on 12×12 lattice. [36]

y -direction, respectively, $p_{i\pm\hat{x}/2,\sigma}^\dagger$ and $p_{i\pm\hat{x}/2,\sigma}$ denote the operators for the p electrons at the site $R_i \pm \hat{x}/2$, and in a similar way $p_{i\pm\hat{y}/2,\sigma}^\dagger$ and $p_{i\pm\hat{y}/2,\sigma}$ are defined. U_d denotes the strength of Coulomb interaction between the d electrons. $u_{i\hat{\mu}}$ and v_i represent the variations of the transfer energy t_{pd} and t_{pp} , respectively. The number of cells which consist of d , p_x and p_y orbitals is denoted as N .

The wave function with the inhomogeneous spin structure is made from solutions of the Hartree-Fock Hamiltonian given as $H_{trial} = H_{pd}^0 + \sum_{i\sigma} [\delta n_{di} - \sigma(-1)^{x_i+y_i} m_i] d_{i\sigma}^\dagger d_{i\sigma}$, where we have variational parameters $\tilde{\epsilon}_p$ and $\tilde{\epsilon}_d$ in H_{pd}^0 . In this paper δn_{di} and m_i are assumed to have the form [29, 30, 31, 32]: $\delta n_{di} = -\sum_j \alpha / \cosh((x_i - x_j^{str}))$, and $m_i = \Delta_{inc} \prod_j \tanh((x_i - x_j^{str}))$, with parameters α and Δ_{inc} where x_j^{str} denote the position of a stripe. The inclusion of stripe order parameters considerably improves the ground-state energy. In small clusters the deviation of the energy of striped state from the exact value is within several percents for the Hubbard model. [33]

The wave function is constructed from the solution of

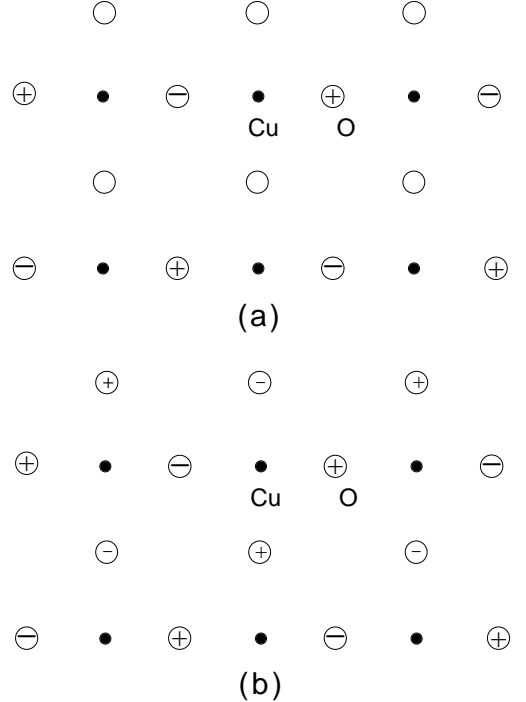


FIG. 3: Lattice structures in the LTT phase (a) and LTO phase (b). The symbol "+" means that the oxygen atoms move upward and instead "-" oxygen atoms move downward. "O" denote the oxygen atom.

Bogoliubov-de Gennes equation given by

$$\sum_j (H_{ij\uparrow} u_j^\lambda + F_{ij} v_j^\lambda) = E^\lambda u_i^\lambda, \quad (3)$$

$$\sum_j (F_{ji}^* u_j^\lambda - H_{ji\downarrow} v_j^\lambda) = E^\lambda v_i^\lambda, \quad (4)$$

where $(H_{ij\sigma})$ and (F_{ij}) are $3N \times 3N$ matrices including the terms for d , p_x and p_y orbitals. The Bogoliubov operators are written in the form

$$\alpha_\lambda = \sum_i (u_i^\lambda a_{i\uparrow} + v_i^\lambda a_{i\downarrow}^\dagger) \quad (E^\lambda > 0), \quad (5)$$

$$\alpha_{\bar{\lambda}} = \sum_i (u_i^{\bar{\lambda}} a_{i\uparrow} + v_i^{\bar{\lambda}} a_{i\downarrow}^\dagger) \quad (E^{\bar{\lambda}} < 0). \quad (6)$$

$a_{i\sigma}$ denotes $d_{i\sigma}$, $p_{i+\hat{x}/2\sigma}$ or $p_{i+\hat{y}/2\sigma}$ corresponding to the components of u_i^λ and v_i^λ .

Then the wave function is written as[34, 35, 36]

$$\begin{aligned} \psi &= P_G P_{N_e} \prod_\lambda \alpha_\lambda \alpha_{\bar{\lambda}}^\dagger |0\rangle \\ &\propto P_G \left\{ \sum_{ij} (U^{-1}V)_{ij} a_{i\uparrow}^\dagger a_{j\downarrow}^\dagger \right\}^{N_e/2} |0\rangle. \end{aligned} \quad (7)$$

U and V are matrices defined by $(V)_{\lambda j} = v_j^\lambda$ and $(U)_{\lambda j} = u_j^\lambda$. P_G is the Gutzwiller operator. The spin modulation potential is contained in $(H_{ij\sigma})$ and the SC order

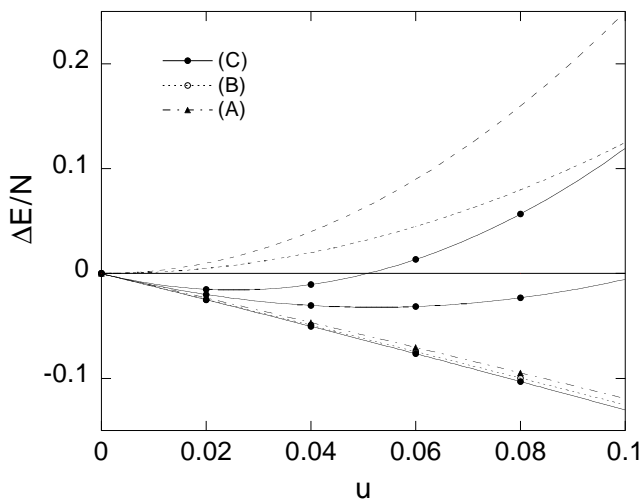


FIG. 4: Energy gain $\Delta E = E(u=0) - E(u)$ ($u = \delta t_{pd}/t_{pd}$) per site as a function of transfer deformation u in t_{pd} units. The parameters are $t_{pp} = 0.4$ and $U_d = 8$ for 16×4 lattice. The hole-rich stripes are in the y -direction. The energy gains for (A) $u_{i\hat{y}} = 0$ (triangles), (B) $u_{i\hat{x}} = 0$, (open circles) and (C) (solid circles) are shown. The elastic energy $Ku^2/2$ is shown by the dashed line (for $K = 5$ and $K = 10$). The summations of $\Delta E = E(u=0) - E(u)$ and the elastic energy per site are also shown for the case (C). The Monte Carlo statistical errors are smaller than the size of symbols.

parameters Δ_{ij} are included in (F_{ij}) . We assume the following spatial variation for the SC order parameters in the d -electron part: $\Delta_{i,i+\hat{x}} = \Delta_s \cos(Q_x(x_i + \hat{x}/2))$, $\Delta_{i,i+\hat{y}} = -\Delta_s \cos(Q_x x_i)$, where $Q_x = 2\pi\delta$ (δ is the hole density). The SC order parameter oscillates according to the spin and charge distributions so that the amplitude has a maximum in the hole-rich region and is suppressed in the hole-poor region. The energy-expectation value is calculated using the Monte Carlo algorithm[6, 11, 15]: $\langle O \rangle = \langle \psi | O | \psi \rangle / \langle \psi | \psi \rangle$.

Here we show the results in the case without lattice distortions. It has been shown that the striped state is more stable than the uniform SDW state for small hole doping.[32] In Fig.1 the size dependence of the SC condensation energy is shown for the uniform SC in the overdoped region and the striped SC in the underdoped region with the results obtained for the one-band Hubbard model for comparison. The parameters are $t_{pp} = 0.4$ and $U_d = 8$ in t_{pd} units. The squares in Fig.1 indicate the SC condensation energy of pure d -wave state at $\delta \approx 0.2$, while the circles are for SC coexisting with stripes at $\delta = 1/8$ for $Q_x = \pi/4$ evaluated on rectangular lattices 32×8 , 24×6 , 16×8 and 16×4 . In both cases the energy obtained through an extrapolation is of the same order as experimental values.

$$E_{cond} \approx 0.00014 t_{pd} \approx 0.2 \text{meV}, \quad (8)$$

where we have assigned $t_{pd} \approx 1.5 \text{eV}$. [37] The data in Fig.2 show the SC condensation energy as a function of the hole density. The SC condensation energy per site for the striped SC is reduced as the hole density decreases, while that for pure d -wave SC remains finite even near half-filling. This suggests that an origin of the decrease of T_c in the underdoped region lies in the reduction of hole-rich domain where the SC order parameter has finite

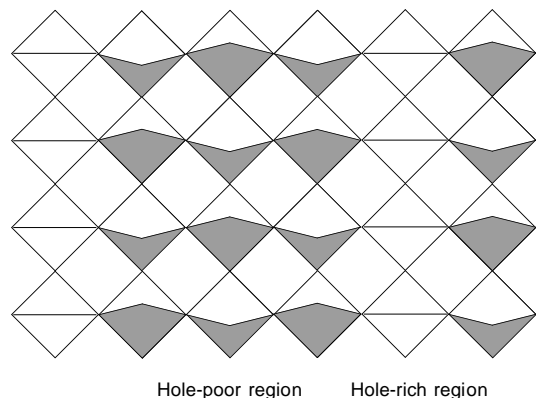


FIG. 5: Schematic structure of lattice distortions and stripes where the hole-rich arrays are perpendicular to the tilting axis. We call this state the mixed LTT-HTT phase. The shaded square represents distorted CuO unit cell.

amplitude.

Now let us consider the effect of lattice distortion on stripes. In the LTT phase stabilized at low temperatures near 1/8-hole filling,[38] the distortions of the CuO square occur in the manner shown in Fig.3. The LTT phase has a 'tilting axis' on which the copper and oxygen atoms never move even in the distorted state.[39] The vertical or horizontal stripes can coexist with the lattice distortions in the LTT phase, being parallel or perpendicular to the tilting axis.

The structural transition from low-temperature orthorhombic (LTO) to LTT phases occurs in LaBaSrCuO and LaNdSrCuO systems.[24] It is not clear a priori what structure is stabilized due to the lattice deformation. We consider the following cases assuming that the stripes are in the y -direction:

- (A) $u_{i\hat{x}} = u, u_{i\hat{y}} = 0, v_i = 0,$
- (B) $u_{i\hat{x}} = 0, u_{i\hat{y}} = u, v_i = 0,$
- (C) $u_{i\hat{x}} = u, u_{i\hat{y}} = u\cos(2Q_x x_i), v_i = u\cos(2Q_x x_i),$

where $Q_x = 2\pi\delta$ and u is the amplitude of deformation: $u_{i\hat{\mu}} = u_{i,-\hat{\mu}}$. $u = 0$ corresponds to the LTO structure, and the anisotropy in t_{pd} indicates a transition to the LTT phase. t_{pd} increases along the tilt axis compared to the LTO phase. The case (C) corresponds to the structure of mixed LTT-HTT phase. The energy gain per site defined as $\Delta E/N = (E(u=0) - E(u))/N$ is presented in Fig.4 as a function of u in t_{pd} units. The energy in the case (B) is lower than that in the case (A) indicating that the stripes are parallel to the tilting axis under the rigid LTT structure. The energy in the case (C) is lower than that in the case (A) indicating that the stripes are parallel to the tilting axis under the rigid LTT structure. We simply assume the same elastic energy cost for these types of rotations. The cost

of energy due to lattice distortions is assumed to be given by $(K/2)u^2$ for the constant K . K is estimated as follows. According to Harrison's rule,[40] t_{pd} is expected to vary as d^{-n} with $n \approx 7/2$, d being the Cu-O bond length. Since $\delta t_{pd}/t_{pd} = -n\delta d/d$, the elastic energy is estimated as

$$E_{el} = \frac{1}{2}C(2d)^3\left(\frac{\delta d}{d}\right)^2 = \frac{1}{2}C(2d)^3\frac{1}{n^2}u^2 \equiv \frac{K}{2}u^2. \quad (9)$$

The constant C is estimated as $C \approx 1.7 \times 10^{12}$ dyn/cm² = 1.7 eV/Å³. [41] Since $d \approx 2\text{Å}$, K is of the order of 10eV: $K \approx 8.9\text{eV}$. We point out that E_{el} has possibly a linear term in u . The θ^2 term, if present in E_{el} , is proportional to u since $u \sim 1 - \cos(\theta) \sim \theta^2/2$ where θ is the tilt angle. The presence of linear term may lead to a first order transition. As shown in Fig.4 the striped state is more stabilized in the LTT phase. We show schematically the stable striped state in the LTT phase in Fig.5 obtained from our VMC evaluations, where the shaded square represents the tilted CuO unit cell rotating around the tilting axis. The LTT-HTT state is more stabilized due to the kinetic energy gain coming from the softening of tilt angles.

In this paper we have investigated the inhomogeneous ground state with the lattice distortions based on the three-band model of high- T_c cuprates using the variational Monte Carlo method. The SC condensation energy decreases as the doping ratio decreases, which is due to the reduction of SC domain in the hole-rich region. The stable striped state has hole-rich arrays being perpendicular to the tilting axis of the lattice distortions in the LTT phase as shown in Fig.5, which can be regarded as the LTT-HTT mixed phase. We thank H. Oyanagi for valuable discussions.

-
- [1] *Proc. of 22nd Int. Conf. Low Temperature Physics* (Helsinki, Finland, 1999) *Physica B***284-288** (2000).
 - [2] N.E. Bickers et al., *Phys. Rev. Lett.* **62**, 961 (1989).
 - [3] C.-H. Pao et al., *Phys. Rev. B***49**, 1586 (1994).
 - [4] P. Monthoux et al., *Phys. Rev. Lett.* **72**, 1874 (1994).
 - [5] T. Nakanishi et al., *J. Phys. Soc. Jpn.* **66**, 294 (1997).
 - [6] K. Yamaji et al., *Physica C* **304**, 225 (1998).
 - [7] J. Kondo, *J. Phys. Soc. Jpn.* **70**, 808 (2001).
 - [8] S. Koikegami and T. Yanagisawa, *J. Phys. Soc. Jpn.* **70**, 3499 (2001); *ibid.* **71**, 671 (2002).
 - [9] K. Yamaji et al., *Physica B***284-288**, 415 (2000).
 - [10] T. Yanagisawa et al., *Physica B***284**, 467 (2000); *ibid.* **B281**, 933 (2000).
 - [11] T. Yanagisawa et al., *Phys. Rev. B***64**, 184509 (2001).
 - [12] J.W. Loram et al., *Phys. Rev. Lett.* **71**, 1740 (1993).
 - [13] P.W. Anderson: *Science* **279**, 1196 (1998).
 - [14] Z. Hao et al., *Phys. Rev. B* **43**, 2844 (1991).
 - [15] T. Yanagisawa et al., *J. Phys. Soc. Jpn.* **67**, 3867 (1998).
 - [16] T. Yanagisawa et al., *J. Phys. Soc. Jpn.* **68**, 3608 (1999).
 - [17] J.M. Tranquada et al., *Nature* **375**, 561 (1995).
 - [18] T. Suzuki et al., *Phys. Rev. B***57**, 3229 (1998).
 - [19] K. Yamada et al., *Phys. Rev. B***57**, 6165 (1998).
 - [20] M. Arai et al., *Phys. Rev. Lett.* **83**, 608 (1999).
 - [21] S. Wakimoto *et al.*, *Phys. Rev. B***61**, 3699 (2000).
 - [22] M. Matsuda *et al.*, *Phys. Rev. B***62**, 9148 (2000).
 - [23] H.A. Mook et al., *Nature* **404**, 729 (2000).
 - [24] N. Ichikawa et al., *Phys. Rev. Lett.* **85**, 1738 (2000).
 - [25] Y.S. Lee et al., *Phys. Rev. B***60**, 3643 (1999).
 - [26] H. Kimura et al., *Phys. Rev. B***59**, 6517 (1999).
 - [27] M. Fujita et al., *Phys. Rev. Lett.* **88**, 167008 (2002).
 - [28] M. Fujita et al., *Phys. Rev. B***65**, 064505 (2002).
 - [29] K. Machida et al., *Phys. Rev. B***30**, 5284 (1984).
 - [30] T. Giamarchi et al., *Phys. Rev. B***42**, 10641 (1990).
 - [31] S.I. Matveenko et al., *Phys. Rev. Lett.* **84**, 6066 (2000).
 - [32] T. Yanagisawa et al., *J. Phys. Condens. Matter* **14**, 21 (2002).
 - [33] T. Yanagisawa et al., private communication.
 - [34] A. Himeda et al., *Phys. Rev. Lett.* **88**, 117001 (2002).
 - [35] T. Yanagisawa et al., *J. Phys. Chem. Solids* **63**, 1379 (2002).

- [36] M. Miyazaki et al., J. Phys. Chem. Solids **63**, 1403 (2002).
- [37] H. Eskes et al., Physica C**160**, 424 (1989).
- [38] T. Suzuki et al., J. Phys. Soc. Jpn. **58**, 1883 (1989).
- [39] A. Bianconi et al., Phys. Rev. Lett. **76**, 3412 (1996).
- [40] W.A. Harrison, *Electronic Structure and Properties of Solids* (Freeman, San Francisco, 1980).
- [41] A. Migliori et al., Phys. Rev. **B41**, 2098 (1990).